

## ORIGINAL PAPER

# Comprehensive Ultrastructure of *Kipferlia bialata* Provides Evidence for Character Evolution within the Fornicata (Excavata)

Naoji Yubuki<sup>a,1</sup>, Alastair G.B. Simpson<sup>b</sup>, and Brian S. Leander<sup>a</sup>

<sup>a</sup>The Departments of Botany and Zoology, Beaty Biodiversity Research Centre and Museum, University of British Columbia, 6270 University Blvd., Vancouver, British Columbia, V6T 1Z4, Canada

<sup>b</sup>Department of Biology, Dalhousie University, Halifax, Nova Scotia, B3H 4R2, Canada

Submitted November 19, 2012; Accepted February 8, 2013  
Monitoring Editor: B. S. C. Leadbeater

***Carpediemonas*-like organisms (CLOs) are important for understanding the evolutionary history of anaerobic excavates (e.g. diplomonads and parabasalids), especially their cytoskeletal traits and the functions of their modified mitochondria (e.g., hydrogenosomes and mitosomes). *Kipferlia bialata* is probably the most commonly encountered CLO and has an intriguing molecular phylogenetic position within the Fornicata; however, this species has yet to be described at the ultrastructural level. This study provides a comprehensive account of the ultrastructure of this excavate using light microscopy, SEM, and serial TEM sectioning. The pattern of flagellar transformation observed with SEM confirms that the posterior basal body is the 'eldest', enabling us to emend the numbering system and associated terminology of the flagellar apparatus in excavates. This revised terminology is fundamental for comparing the cytoskeletons of the Excavata supergroup with other eukaryotes. Moreover, *K. bialata* had several unusual features, such as a hood, a distinct gutter within the ventral groove, and hairs along a single flagellar vane. The ultrastructural data reported here significantly improve our understanding of fornicate morphology, and when placed within a molecular phylogenetic context, these data shed light onto patterns of character evolution within the Excavata.**

© 2013 Elsevier GmbH. All rights reserved.

**Key words:** *Carpediemonas*-like organisms; cell division; cytoskeleton; flagellar apparatus; microtubules; ultrastructure.

---

<sup>1</sup>Corresponding author. fax +1 604 822 6089  
e-mail yubuki@mail.ubc.ca (N. Yubuki).

**Abbreviations:** A, A fiber; B, B fiber; B1, basal body 1; B2, basal body 2; B3, non-flagellated basal body 3; B4, non-flagellated basal body 4; Ba, bacterium; C, C fiber; CLO, *Carpediemonas*-like organism; Cy, cytopharynx; F1, flagellum 1; F2, flagellum 2; G, gutter; Gr, ventral groove; H, hood; I, I fiber; IDR, inner root 2-associated dense rod; iR2, inner root 2; ODR, outer root 2-associated dense rod; oR2, outer root 2; MRO, mitochondrion-related organelles; N, nucleus; R1, root 1; R2, root 2; R3, root 3; S, singlet root.

## Introduction

The Fornicata (Excavata; Metamonada) is a group of heterotrophic flagellates with diverse modes of life in low oxygen environments, including both parasites and free-living species. The taxon includes two long-known, mostly parasitic groups – diplomonads (e.g. *Giardia*, *Spironucleus*) and retortamonads (e.g. *Retortamonas*), plus a very little-studied but diverse assemblage of free-living forms called the ‘*Carpediemonas*-like organisms’, or CLOs. Diplomonads, in particular, were once thought to lack mitochondria and to have diverged from other eukaryotes prior to the origin of mitochondria, under the so-called “Archezoa hypothesis” (Cavalier-Smith 1983; Roger et al. 1999; Sogin 1991; Sogin et al. 1989). However, it is now understood that the deep phylogenetic position of diplomonads and other lineages of unusual parasites in trees inferred from sequences such as ribosomal DNA is a long-branch-attraction artifact (Philippe and Germot 2000; Philippe et al. 2000). Moreover, highly reduced mitochondrion-related organelles (MROs, e.g., mitosomes) have been discovered in the diplomonad *Giardia intestinalis* (and other lineages of unusual parasites), suggesting that mitochondria were acquired prior to the most recent ancestor of all extant eukaryotes (Embley and Martin 2006; Hampl and Simpson, 2008; Hjort et al. 2010; Simpson and Patterson 1999; Simpson et al. 2000; Tovar et al. 2003).

Recent studies show that *Carpediemonas*-like organisms (CLOs), which were almost unknown a decade ago, represent most of the major-lineage-level diversity of fornicates and are key to understanding the evolution of the group. There are currently five different genera of CLOs, plus some undescribed forms, that represent at least six major lineages, termed CL1-6 (Kolisko et al. 2010; Park et al. 2010). These are *Dysnectes* (CL1), an undescribed *Carpediemonas*-like organism (CL2), *Hicanonectes* and relatives (CL3), *Carpediemonas* itself (CL4), *Ergobibamus* (CL5), and *Kipferlia* (CL6). A representative of each of CL1, CL3, CL4 and CL5 has been described at the ultrastructural level (Park et al. 2009, 2010; Simpson and Patterson 1999; Yubuki et al. 2007); CL2 and CL6 have only been characterised with light microscopy (LM) and small subunit (SSU) rDNA sequences (Kolisko et al. 2010; Takishita et al. 2012).

Molecular phylogenetic analyses of the Fornicata have demonstrated that (i) retortamonads (*Retortamonas* and *Chilomastix*) are either

polyphyletic or deeply paraphyletic, (ii) *Dysnectes* (CL1) is the free-living sister lineage to a clade consisting of (parasitic/commensal) diplomonads and *Retortamonas*, and (iii) *Kipferlia* (CL6) is positioned between *Chilomastix* and the *Dysnectes*/diplomonad/*Retortamonas* clade (Takishita et al. 2012). Therefore, *Kipferlia*, along with *Dysnectes* is a particularly important lineage for understanding character evolution within the Fornicata, especially switches from free-living to parasitic modes of life and the transition from hydrogenosome-like organelles to mitosomes.

Kolisko et al. (2010) created the genus *Kipferlia* for the organism that was originally described as *Cryptobia bialata* Ruinen, 1938, and was later renamed *Carpediemonas bialata* (Ruien) Lee and Patterson, 2000. The genus *Kipferlia* was established because molecular phylogenies showed that this lineage was only distantly related to *Carpediemonas membranifera*, the type species for *Carpediemonas* (CL4) (Kolisko et al. 2010; Takishita et al. 2007, 2012; see above). Eleven different cultures and 14 SSU rDNA sequences of *Kipferlia bialata* have been reported from all over the world (Berney et al. 2004; Edgcomb et al. 2002; Kolisko et al. 2010; Lee 2002, 2006; Lee and Patterson 2000; Takishita et al. 2007); these are high numbers when compared to the other CLO clades, which are currently represented by only one or two different cultures and (usually) no environmental SSU rDNA clones (Kolisko et al. 2010). Therefore, *K. bialata* could be widespread and perhaps relatively abundant in low oxygen sediments.

Despite the repeated observations of *K. bialata* (CL6) and its important phylogenetic position, almost nothing is known about the ultrastructure of the cell. Here we describe in detail the cellular architecture of *K. bialata* (strain NY0173), paying particular attention to the flagellar apparatus. We resolve the pattern of flagellar transformation in the dividing cell, and establish a hypothetical framework for understanding character evolution within CLOs and the Fornicata as a whole.

## Results

The morphology of *K. bialata* NY0173 was characterized with light microscopy (Fig. 1), SEM (Figs 2-3), and serial TEM sections at different angles (Figs 4-8). A reconstruction of the overall flagellar apparatus of *K. bialata* was shown in Figure 9.

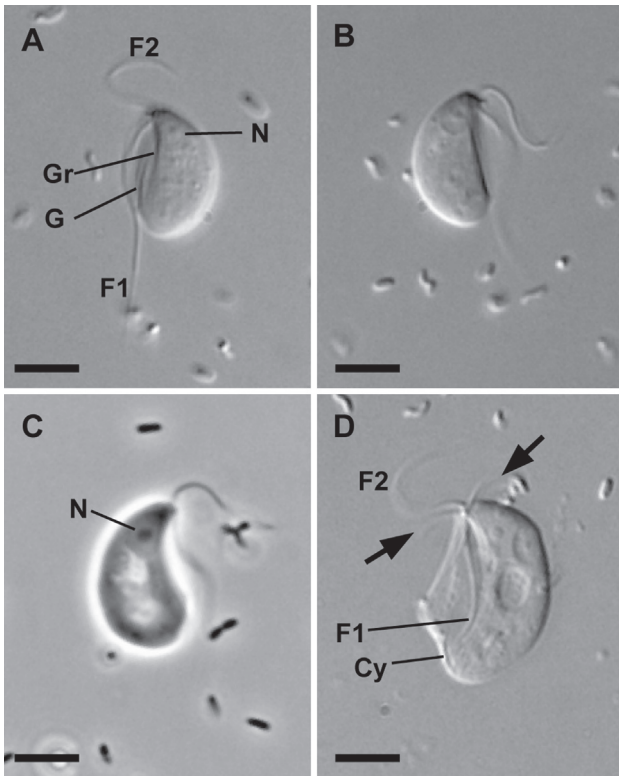


**Figure 1.** Light micrographs of *Kipferlia bialata*. Scale bar: 5  $\mu\text{m}$ . **A, B, D.** Differential interference contrast light micrographs showing the two flagella (F1 and F2), a deep gutter (G) within the ventral groove (Gr), and newly developing flagella (arrows) and cytopharynx (Cy) on a compressed cell in D. **C.** Phase contrast light micrograph showing the nucleus (N) positioned in the anterior region of the cell.

### General Morphology of *Kipferlia bialata* NY0173

The general morphology of the isolate of *K. bialata* examined in this study corresponded with the taxonomic diagnosis in a previous report (Kolisko et al. 2010). Each cell had two flagella and a ventral groove for capturing and consuming bacteria (Fig. 1). Cells were usually bean-shaped and measured 12.9  $\mu\text{m}$  (10.4–17.7  $\mu\text{m}$ ) long and 6.5  $\mu\text{m}$  (5.4–7.8  $\mu\text{m}$ ) wide ( $n=30$ ) when viewed live with light microscopy. The isolate swam slowly and often adhered to the surface of the substrate while rapidly beating the anterior flagellum. The two flagella emerged subapically from the ventral side of the cell. Flagellum 1 (F1) was approximately 1.5 times the length of the cell, moved in a sinuous pattern, and was directed posteriorly, within the ventral groove (Fig. 1). This flagellum possessed a single broad vane on its ventral-most side

that was clearly seen only by electron microscopy, and that was extended by a terminal row of hairs (Figs 2C and E–H, 4A, B and D). Flagellum 2 (F2) extended anteriorly and was nearly the same length as the cell (Fig. 1). A membranous “hood” covered the anterior region of the cell above the F1 insertion and extended down the left and right margins of the ventral groove; the hood extended about three quarters of the cell down the right margin of the groove, and 1.5–2  $\mu\text{m}$  down the left margin of the groove (Fig. 2A–B). The inner lining of the groove was supported by microtubules and fibers (Fig. 2D). The bottom of the groove formed a deep “gutter” that led into a conspicuous “cytopharynx” at the posterior region for the engulfment of bacterial prey cells (Fig. 2E–H). The nucleus was located in the anterior region of the cell close to the flagellar apparatus (Figs 1, 4A and B). The cells also possessed rounded mitochondria-related organelles (MRO) about 500 nm in diameter that were bounded by two closely addressed membranes, contained a dense matrix and lacked cristae (Fig. 4C, F and G). No discrete Golgi apparatus was observed.

### Flagellar Transformation as Viewed with SEM

In preparation for cell division, two new flagella emerged near the two parental flagella, F1 and F2 (Figs 1D, 2D, 3A–B). F1 was distinguished from F2 by the presence of the longitudinal vane and the orientation toward the posterior end of the cell (see above). The two nascent flagella elongated to form two F2 flagella, without vanes, designated as “F2a” and “F2b” (Fig. 3C–E). The parental F2 flagellum simultaneously transformed into a new F1 flagellum, designated as “F1\*”, by developing a vane and reorienting toward the posterior end of the cell in association with a new ventral groove (Fig. 3C–E). The original F1 flagellum meanwhile maintained its length, its vane and its position at the head of the old ventral groove. At this stage of cytokinesis, the cell contained two ventral grooves, two nascent F2 flagella (F2a and F2b), and two fully elongated F1 flagella (F1 and F1\*) (Fig. 3D). Each F1 flagellum became paired with one of the nascent F2 flagella during late stages of cytokinesis; one daughter cell received F1 and F2a; the other daughter cell received F1\* and F2b (Fig. 3E). In other words, each daughter cell inherited one of the nascent F2 flagella and one of the parental flagella (F1 and F1\*). The flagella in *K. bialata* were therefore inherited in a semi-conservative pattern whereby the posterior F1 flagellum was older than the anterior F2 flagellum in each interphase cell.



**Figure 2.** Scanning electron micrographs (SEM) of *Kipferlia bialata*. Arrows in A, B & D denote the posterior termination points of the hood (H). **A-B.** Ventral view showing the two flagella (F1 and F2), a deep gutter (G) within the ventral groove (Gr) and the posterior position of the cytopharynx (Cy). Scale bars: 1.5  $\mu\text{m}$  for A, and 2  $\mu\text{m}$  for B. **C.** High-magnification view of F1 showing the ventral flagellar vane (V) and associated hairs. Scale bar: 500 nm. **D.** Cell with most of the plasma membrane removed revealing the underlying microtubules and posterior position of the cytopharynx (Cy). Note the number of microtubules supporting the right side of the gutter (G) is reduced near the termination of the hood (arrow on left side of the micrograph). Scale bar: 2  $\mu\text{m}$ . **E-H.** A series of images showing the engulfment of bacteria (Ba) through cytopharynx (Cy) located in the posterior region of the gutter (G). Scale bars: 2  $\mu\text{m}$ .

### Organization of the Flagellar Apparatus

The overall organization of the flagellar apparatus in *K. bialata* was similar to other CLOs studied previously (Park et al. 2009, 2010; Simpson and Patterson 1999; Yubuki et al. 2007); however, we applied a revised set of terms for the microtubular roots, basal bodies, and flagella of *K. bialata* based on the original proposals by Moestrup (2000) for a universal terminology for eukaryotes.

**Overview.** Four basal bodies were present in most (interphase) cells; however, only two basal bodies were observed in a few cells, presumably newly formed daughter cells. The posterior basal body, B1, and the anterior basal body, B2, gave rise to F1 and F2, respectively, and were arranged almost perpendicularly with the proximal end of B1 almost abutting the side of B2 (Fig. 5A-D). B1 and B2 were connected to their associated flagella via transitional plates which

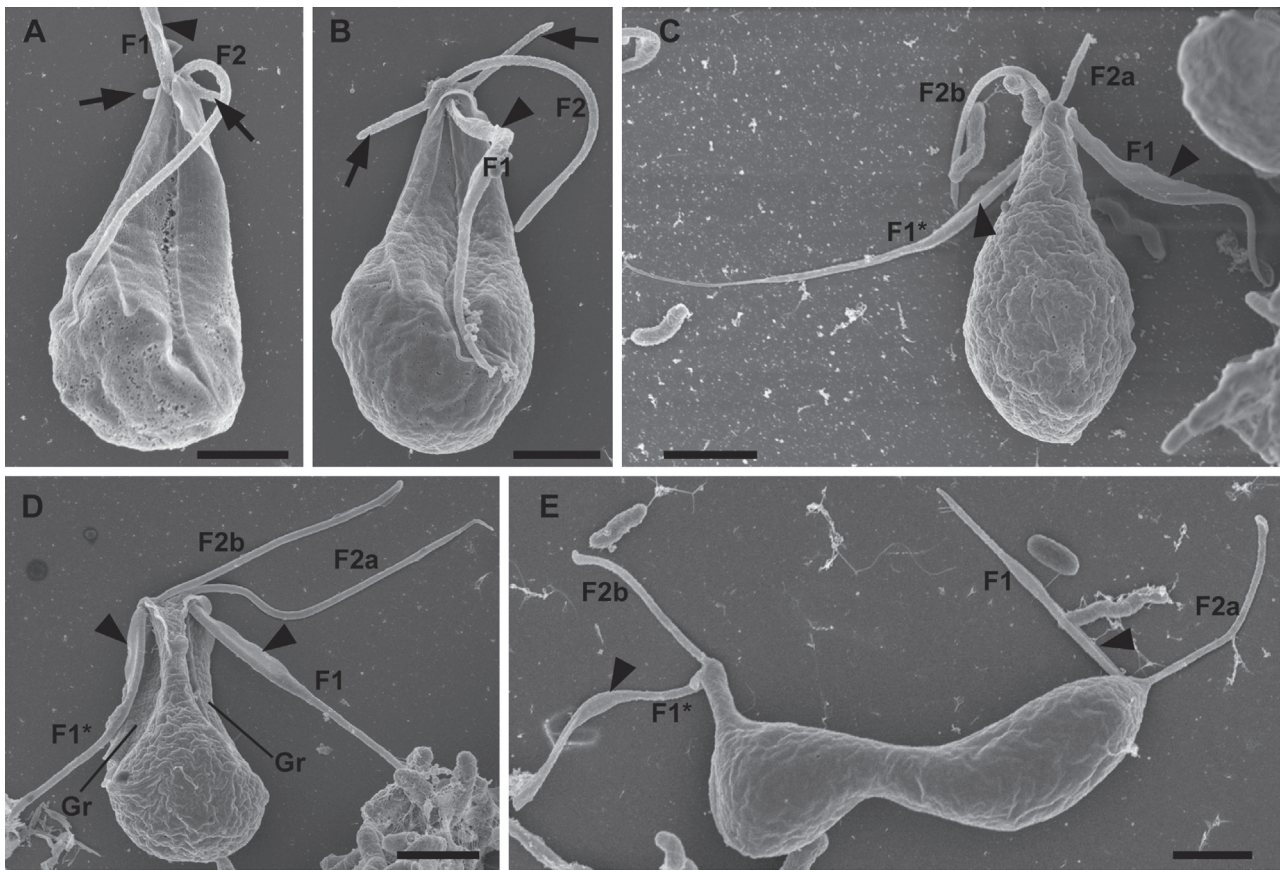


**Figure 3.** Scanning electron micrographs (SEM) showing flagellar transformation in *Kipferlia bialata*. Arrowheads indicate the ventral vanes on F1 and F1\*. **A-B.** SEMs showing two new flagella (arrows) emerging near the two parental flagella (F1 and F2). The insertion point and presence of a longitudinal vane distinguishes F1 from F2. **C.** SEM showing two shorter nascent flagella (F2a and F2b) and two longer flagella with vanes; “F1\*” refers to the parental F2 flagellum that has transformed into a new F1 flagellum. **D.** SEM showing a cell with two ventral grooves (Gr) and two fully elongated F2 flagella, “F2a” and “F2b”. Flagella F1 and F1\* both have vanes (arrowheads). **E.** SEM of a cell in a late stage of cytokinesis showing the segregation of F1 and F2 flagellar pairings. One daughter cell receives F1 and F2a; the other daughter cell receives F1\* and F2b. Scale bars: 2  $\mu\text{m}$ .

were ‘buried’ deeper within the cell than the flagellar insertion points (Fig. 5C-D). Three microtubular roots extended from B1, namely R1, R2, and a singlet root (S) (Figs 5F, G, 6A-C). One root, R3, originated from B2 (Fig. 5C-D). Three major fibers were associated with R2, namely the A fiber, B fiber, and I fiber while a comb-like “C fiber” and part of the B fiber were associated with R1 (Figs 5F-G, 6B-C, 7A-C). Two auxiliary basal bodies, B3 and B4, were positioned on the left and right sides of the B1/B2 axis, respectively, and directed laterally (Fig. 6A-B). B3 was positioned near microtubular root R3, and dorsal to R1 (Figs 5H, 6A-B); B4 was situated within the concave ventral face of microtubular root R2 (Figs 5E, 6B).

**Root 1, and associated structures, and singlet root:** R1 originated from the left-ventral side of B1 and extended posteriorly (Fig. 5). Up to six microtubules were added to the left side of R1 as it moved away from B1 (Fig. 5E-H). The C fiber appears comb-like in transverse section and was associated with the dorsal side of R1 from its origin (Fig. 5A-B, F-H). Each vane-like component of the C fiber extended from the R1 microtubules and joined together into one thick darkly stained sheet, which connected up with the left end of the A fiber (Figs 5F-H, 6B). The C fiber terminated near the level of the F1 insertion (Figs 5A, 6C-D, 7B-D). The B fiber (see below) connected to the ventral side of R1 at its origin, and continued posteriorly with R1 for some distance (Figs 5, 6A-D, 7). R1 and

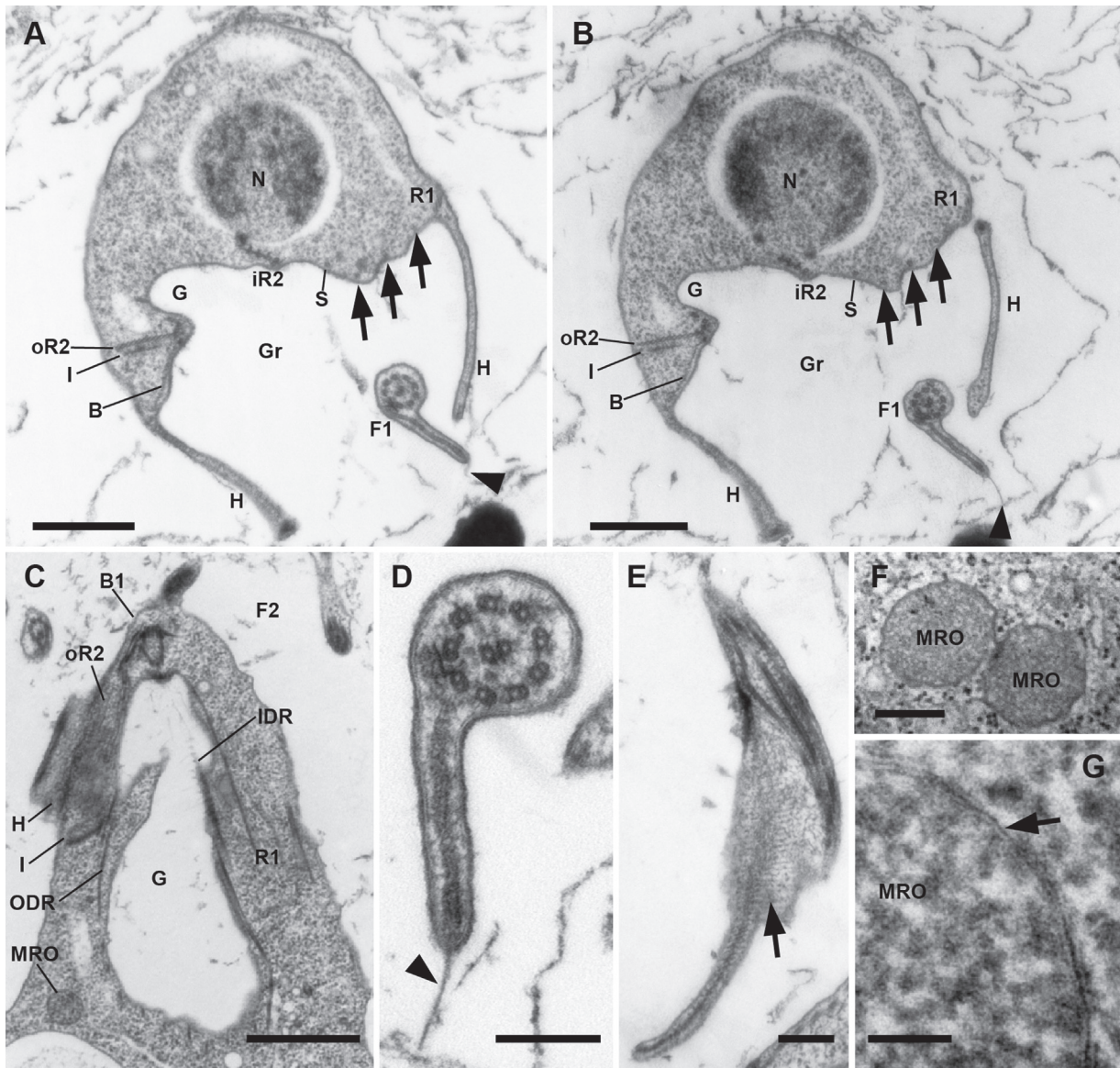


**Figure 4.** Transmission electron micrographs (TEM) of *Kipferlia bialata*. **A-B.** Transverse section through the anterior part of the cell showing the nucleus (N) and the F1 flagellum viewed from the anterior side of the cell. The hood (H) extends posteriorly. Both margins of the deep gutter (G) are within the ventral groove (Gr). Note three microtubules split away from the right side of R1 (arrows). Arrowheads indicate the hairs on the vane of F1. Scale bars: 1  $\mu\text{m}$ . **C.** Section through the anterior part of the cell. The inner root 2-associated dense rod (IDR) supports the left margin of the gutter (G). Scale bar: 2  $\mu\text{m}$ . **D.** High magnification view showing the ventral flagellar vane on F1 and the associated hairs (arrowhead). Scale bar: 200 nm. **E.** Grazing section of F1 showing striation of the vane (arrow). Scale bar: 500 nm. **F.** Mitochondria-related organelles (MRO) preserved by conventional chemical fixation. Scale bar: 250 nm. **G.** High magnification view of the MRO showing two enveloping membranes (arrow). Scale bar: 50 nm.

this leftwards extension of the B fiber supported the base of the left side of the hood near the F1 insertion. The microtubules of R1 split away individually from its right side to support the left side of the ventral groove (Figs 4A-B, 7D-I, 9). The singlet root (S) originated from alongside the dorsal

side of B1, near the dorsal/left face of R2 and ran along the ventral groove toward the posterior end of the cell (Figs 5F-H, 6B-F, 7), immediately to the right of the microtubules that originated from R1 (Figs 4A-B, 7F-I). The loose band formed by the R1-derived microtubules and S continued

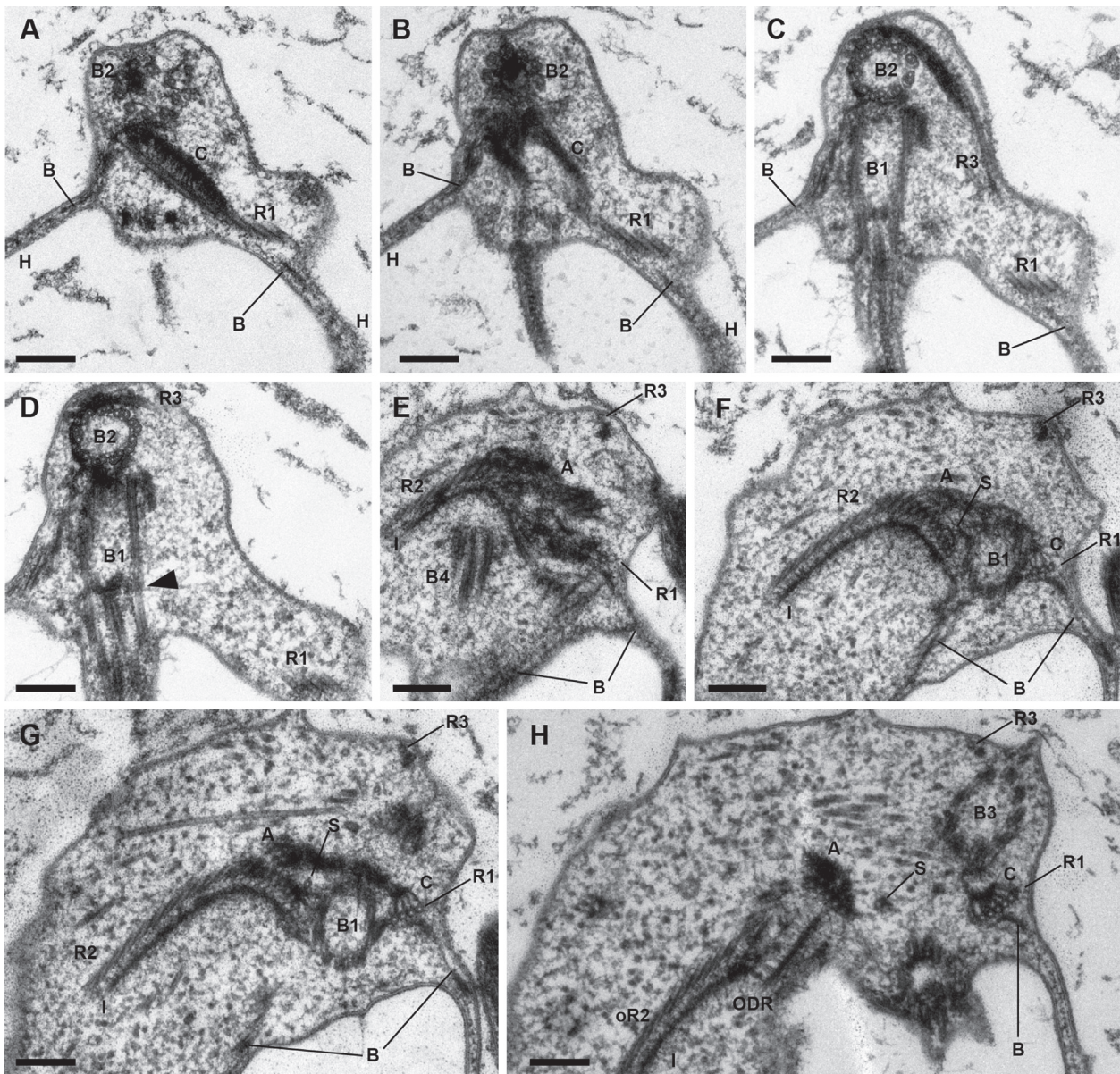


**Figure 5.** Transmission electron micrographs (TEM) of *Kipterlia bialata* showing root 1 (R1), root 3 (R3) and the C fiber (C). Scale bars: 200 nm. **A-D.** Non-consecutive serial sections viewed from the left anterior side of the cell. **A.** A grazing section of the comb-like C fiber on R1. **B.** A section showing traces of the C fiber and R1. **C.** A dense fiber runs along R3 and originates from the dorsal side of basal body 2 (B2). Note B1 and B2 are arranged perpendicularly. **D.** R3 originates from the dorsal side of B2. The arrowhead indicates the transitional region between the flagellum and the basal body. **E-H.** Non-consecutive serial sections viewed from the anterior side of the cell. **E.** Two microtubules of R1 can be seen at the proximal area of B1. R3 runs under the cell membrane and is closely related with an electron dense fiber. **F.** Three microtubules of R1, with a comb-like C fiber elements extending from each R1 microtubule. **G.** TEM showing four microtubules of R1, and four comb-like extensions and dark layer of C fiber. The B fiber is also associated with the ventral side of R1, and the A fiber extends from the C fiber to R2 on the dorsal side of B1. Internal microtubules are positioned behind B1 and R2. **H.** TEM showing six microtubules of R1 and six comb-like extensions of the C fiber. Note that the dark layer associated with the C fiber and R3 is connected to the auxiliary basal body 3 (B3).

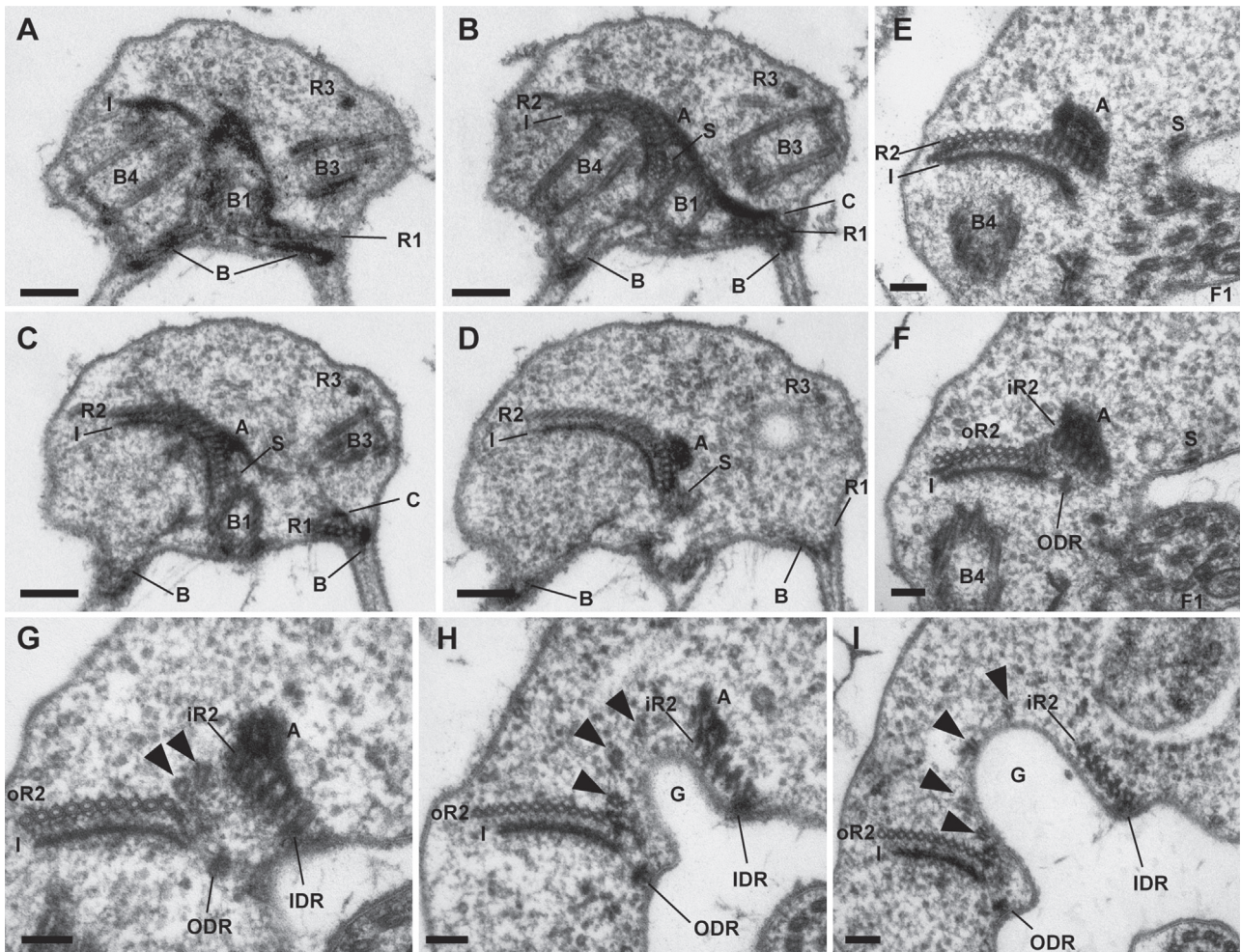


**Figure 6.** Transmission electron micrographs (TEM) of *Kipferlia bialata* showing root 2 (R2), the A fiber (A), and the I fiber (I). All images are viewed from anterior end of the cell. **A-D.** Non-consecutive serial sections. Scale bars: 200 nm. **A.** The B fiber stretches from right to left along the groove on the ventral side of B1. **B.** The A fiber links to the dorsal side of R2, B1 and the C fiber. B3 is located to the dorsal side of the C fiber, and B4 is located on the concave face of R2. R3 is close to B3. **C.** The width of the A fiber is reduced toward R2. **D.** The A fiber is positioned on the left side of R2. **E-I.** Non-consecutive serial sections. Note the A fiber is located on the dorsal side of iR2 as a dense body, and oR2 has short dorsal projections on each microtubule. Scale bars: 100 nm. **E.** TEM of a cell prior to the separation of R2. **F.** R2 is split into two bands: six microtubules form the inner band (iR2) and 11 microtubules form the outer band (oR2). The outer root 2-associated dense rod (ODR) is located on the ventral side of iR2. **G.** The oR2 includes 12 microtubules. Two left microtubules (arrowheads) are disassociated with oR2. The I fiber is cross-linked with the ventral side of oR2. **H.** TEM showing 15 microtubules of oR2. The gutter (G) invaginates between the inner root 2-associated dense rod (IDR) and the ODR. Three microtubules (arrowheads) from oR2 support the wall of the gutter. **I.** TEM showing 16 microtubules of oR2, including four (arrowheads) that support the wall of the gutter (G).

posteriorly for most of the length of the cell and terminated in association with the forming cytopharynx (see Fig. 2D).

**Root 2 and associated structures:** R2 was the major cytoskeletal element supporting the ventral groove. It originated against the dorsal side of B1, and near its origin consisted of a single row of 15-16 microtubules that curved rightwards

(Figs 5E-G, 6A-D). The right portion of the A fiber was associated with the dorsal side of the 'inner' portion of R2, thus linking the R2 and C fiber around the dorsal side of B1 (Figs 5E-G, 6B-D). The I fiber was a latticed structure with an distinct sheet-like ventral face that was cross-linked with the ventral face of R2 (Figs 5E-H, 6, 7). The ventral face of the I fiber was associated with the auxiliary B4

(Fig. 6A-B). Near the F1 insertion, the microtubules of R2 split into two different branches: an inner R2 (iR2) of 5-6 microtubules and an outer R2 (oR2) with the remaining ~10 (Figs 6E-I, 7A-B). The thick portion of the A fiber continued with the right portion of iR2 for a short distance before terminating, while the I fiber continued with oR2 only (Figs 6D-I, 7A-G). Remnants of the A fiber were associated with the dorsal side of the proximal portion of oR2, appearing as short projections from each microtubule (Fig. 6F-I).

As they diverged, the region between iR2 and oR2 formed a deep gutter (G) (Figs 6G-I, 7D-F). The margins of this gutter were framed by similar, non-microtubular fibers about the same size as an individual microtubule – the inner root 2-associated dense rod (IDR) and the outer root 2-associated dense rod (ODR) (Fig. 6D-I). Both IDR and ODR originate against the inner/left/ventral edge of iR2 (Figs 5H, 7C, F) and ODR at least is likely homologous to the RDR of *Carpediemonas membranifera* (Simpson and Patterson 1999). The left side of the gutter was supported by the iR2 and IDR (Figs 6H-I, 7D-I). The right side of the gutter was supported by the ODR, plus the left edge of oR2 and the connected I fiber (Figs 6F-I, 7D-I).

The two margins of the gutter were clearly visible under the SEM, especially in cells with the plasma membrane removed (Fig. 2A-B, D-H). The IDR extended all the way to the cytopharynx (Figs 2D, 8). The ODR terminated seemingly before the origin of the cytopharynx (though see description of the ‘composite fiber’ below). Several microtubules from the left side of oR2 disassociated with one another to reinforce the walls and ‘floor’ of the gutter (Figs 6G-I, 7D-I). Approximately five extra microtubules were added consecutively, one by one, to the right side of oR2 until the total number of oR2 microtubules reached at least 16 (Fig. 6I).

**The B fiber supports the hood:** The B fiber arched around the ventral side of B1 and connected with R1 on the left side of the groove, and with the I fiber and the left side of R2 on the right (Figs 5E-F, 7A-C). The B fiber was extended in width to cover a wide area as a thin sheet with a thickened edge and ultimately formed the main support for the hood. The B fiber and hood extended posteriorly to (initially at least) reinforce both margins of the ventral groove (Figs 4A-C, 5, 7), with the thickened edge of the B fiber supporting the margin of the hood, especially on the right side of the groove (Fig. 4A-C). As noted above, the left extension of hood was relatively short.

**Root 3 and the associated fiber:** R3 consisted of a single microtubule and originated from the

anterior side of B2 (Figs 5C-H, 6A-D). R3 was closely associated with a dense fiber along its entire length and extended toward the left side of the cell in the vicinity of B3. R3 was not associated with additional microtubules or a distinct dorsal fan. However, a number of individual microtubules originated from near the base of B2 and B3, and extended dorsally and posteriorly, with some of them apparently supporting the dorsal cell membrane (Fig. 5 E-H).

## Cytopharynx

In the posterior portion of the ventral groove the deep gutter extended to form the cytopharynx, which was also supported by microtubules and fibers derived from R2 (Figs 2A-B, D, 8A-B). About three quarters of the way down the cell there was a marked change in the structure of the right side of the ventral groove: The right branch of the hood terminated, while the dense portion of the ‘composite fiber’ (see below) arose from near the end of the base of the hood (Figs 2A-B, D, 8C-H). It was possible, but not demonstrated, that this dense portion was a thickened extension of the ODR. At about the same point the striated portion of the composite fiber originated on the cytoplasmic side of the leftmost oR2 microtubules (Fig. 8C-H). More posteriorly the dense portion angled leftward to join up with the striated portion, and as it did so, the rightmost majority of the oR2 microtubules terminated against the dense portion (Figs 2D, 8C-F). The remaining oR2 and iR2 microtubules supported the posterior region of the cytopharynx (Fig. 8G-O), and became associated with the composite fiber, which specifically supported the right side of the cytopharynx (Fig. 8A-I). The IDR and iR2 continued to support the left edge of the cytopharynx; these fibers reinforced the outline of the cytopharynx and were visible with the SEM (Fig. 2A-B, D). The number of microtubules in oR2 decreased gradually toward the posterior end of the ventral groove, which became narrower as the cytopharynx curved toward the left (Fig. 8K-O).

## Discussion

### Amending the Terminology for the Excavate Flagellar Apparatus

The overall organization of the eukaryotic cytoskeleton is highly conserved, so modifications of cytoskeletal traits associated with the flagellar apparatus distinguish major groups of eukaryotes and inform protistan systematics (Andersen 1991;

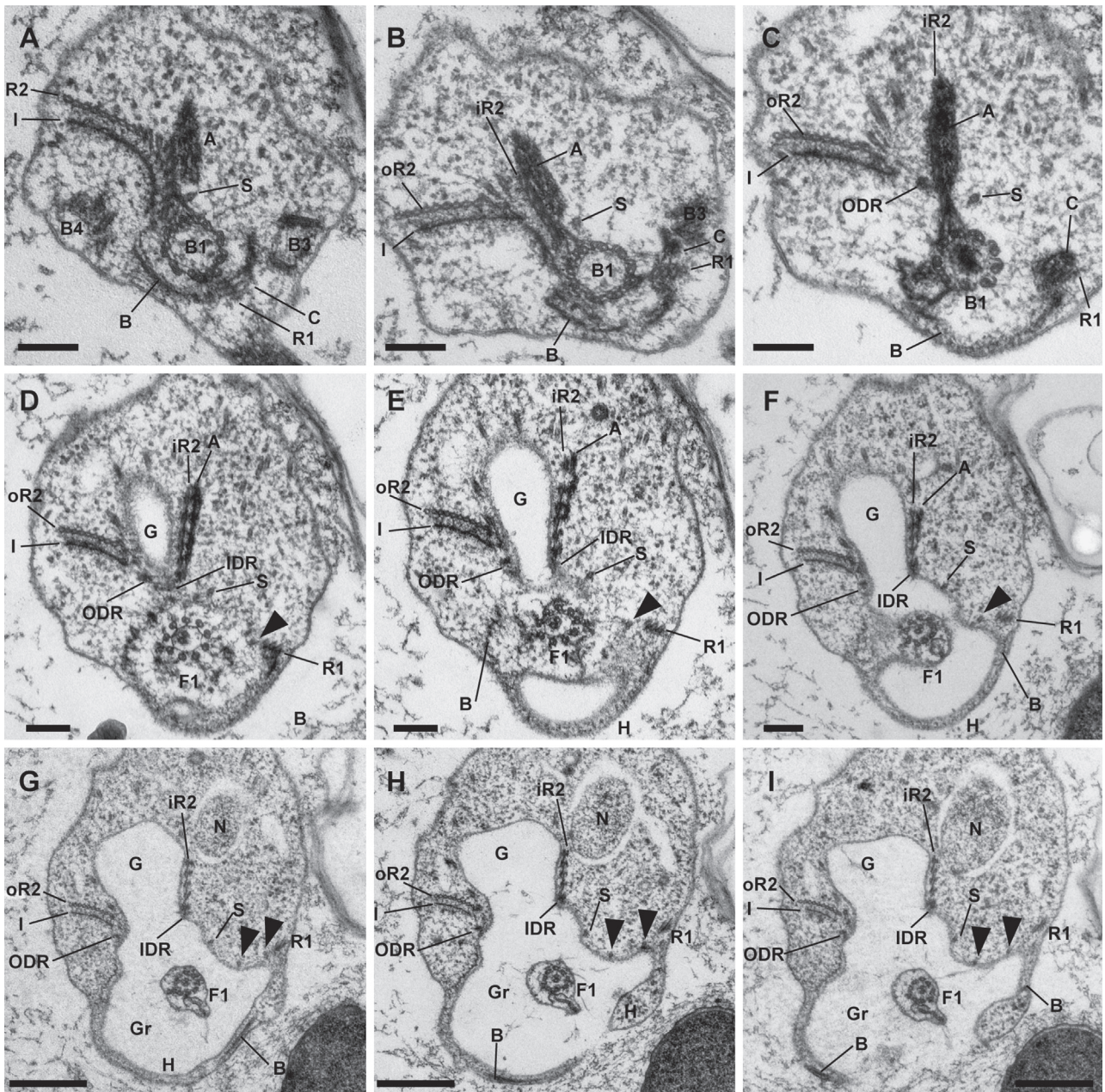


**Figure 7.** Non-consecutive serial TEM sections of *Kipferlia bialata* showing the B fiber and the hood. Arrowheads in D-I indicate microtubules that are derived from the right side of R1. Scale bars: 200 nm for A-F, and 500 nm for G-I. **A-B.** The B fiber arches from R1 to R2 against B1. **C.** TEM showing the transitional region between B1 and F1. ODR originates near iR2. **D.** TEM showing the origin of the gutter (G). **E.** TEM showing the origin of the hood (H). The B fiber supports the hood. **F-G.** TEM showing the B fiber associated with the ODR on the right side of the gutter (G). **H-I.** The hood extends posteriorly down the right and left margins of the ventral groove (Gr).

Beech et al. 1991; Moestrup 1982, 2000; Sleight 1988). Moestrup (2000) proposed a universal terminology for the basal bodies and flagellar microtubular roots of eukaryotes, focusing primarily on algal groups. This account considered the

flagellar apparatuses of the Euglenozoa, which includes euglenophycean algae, but did not consider other excavates. Moestrup's (2000) labelling for euglenozoans, however, included what appears to be an error; the identities for the microtubular

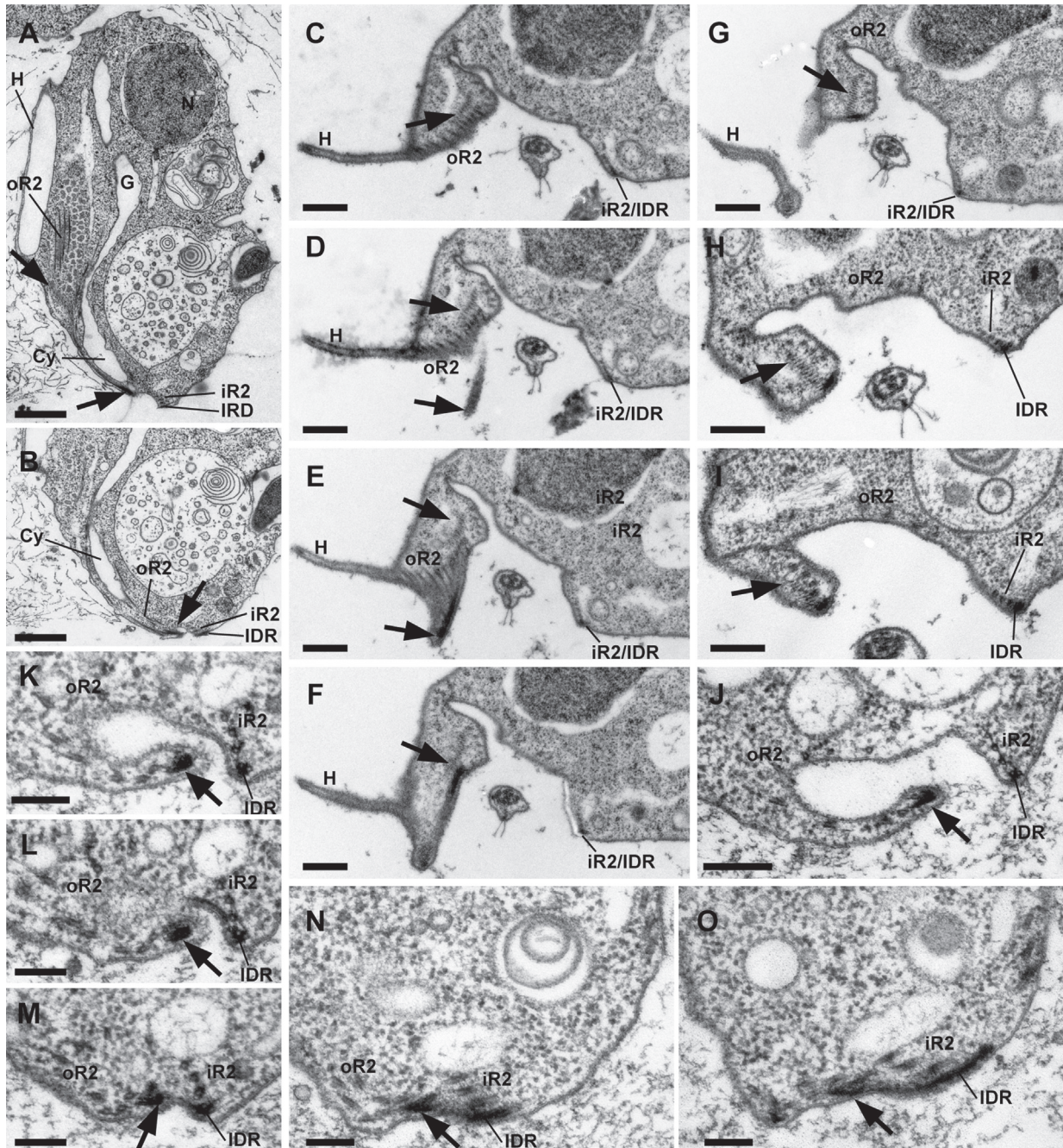


**Figure 8.** Transmission electron micrographs (TEM) of *Kipferlia bialata* showing cytopharynx and supporting structures. Arrows indicate composite fiber. **A-B.** Non-consecutive serial TEM sections of the cell. The curved cytopharynx (Cy) is supported by the oR2, composite fiber, iR2 and IDR. Scale bars: 1  $\mu\text{m}$ . **C-I.** Non-consecutive serial sections of the cell. Scale bars: 500 nm. **C-D.** TEM showing the striated portion of the composite fiber located behind oR2. **E.** TEM showing the the right part of oR2 terminating at the dense portion of the composite fiber. The rest of the oR2 supports the wall of the cytopharynx. **F-G.** TEM showing the termination of the hood. **H-I.** TEM showing the the right and left edge of the cytopharynx being supported by the composite fiber and IDR, respectively. **J-O.** Non-consecutive serial sections of the posterior end of the cell. Scale bars: 200 nm. **J.** TEM showing that the composite fiber and IDR are situated at the margins of the cytopharynx. **K-L.** TEM showing the cytopharynx reducing in size. **M-O.** TEM showing that the oR2, iR2, composite fiber and IDR continue to run under the cell membrane and curve toward the left.

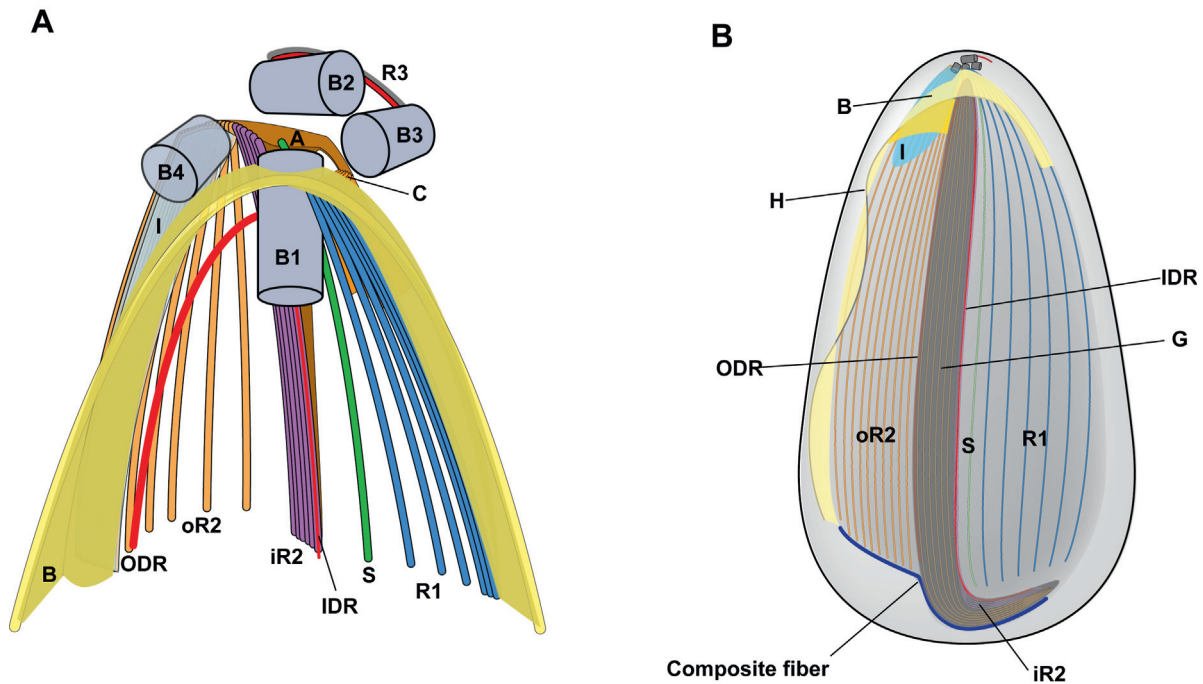


**Figure 9.** Illustration of the flagellar apparatus of *Kipferlia bialata* based on the electron micrographs in the preceding plates. **A.** Detailed organization of the anterior area. **B.** Overall organization of the microtubular cytoskeleton supporting the ventral groove.

roots for each basal body were inverted relative to the other taxa considered in the comparative study (see below). Simpson (2003) then attempted to extend Moestrup's universal terminology to cover the flagellar apparatuses of all excavates, but did so by comparison with the Euglenozoa, and not other taxa. Unfortunately this propagated the likely-incorrect terminology for the Euglenozoa to all excavates. Furthermore, Simpson's (2003) comparison of 'typical excavates' to euglenozoans was based almost entirely on comparisons of interphase cells, whereas identification of homologies according to Moestrup's (2000) system ultimately relies on developmental information associated with the replication of the flagellar apparatus. An examination of the highly derived diplomonad *Giardia* demonstrated a developmental pattern in which the posterior-most 'caudal flagella' represented the ultimate stages (Nohýnková et al. 2006). Until the current study, however, there has been almost no data on flagellar apparatus replication in typical excavates, aside from a brief textual account on jakobids by O'Kelly (1993). Given these problems, recent studies of CLO ultrastructure have reverted to naming microtubular roots by position, for example, with the major roots on the left side and right side of the ventral groove being called the 'left

root', and 'right root' respectively (Park et al. 2009, 2010; Yubuki et al. 2007).

We have reviewed the universal terminology for biflagellates proposed by Moestrup (2000, p. 71) to characterize the excavates compared in this study:

- (i) The older flagellum is identified as "flagellum 1";
- (ii) The younger flagellum is identified as "flagellum 2";
- (iii) The two microtubular roots associated with flagellum 1 are identified as "root 1" and "root 2";
- (iv) The two microtubular roots associated with flagellum 2 (where present) are identified as "root 3" and "root 4";
- (v) The roots are identified in a clockwise fashion, looking down the basal body from the outside of the cell;
- (vi) The following changes to the microtubular roots occur during the transformation of the younger flagellum 2 into a mature flagellum 1 during cell division: root 3 becomes root 1, and root 4 becomes root 2. In other words, root 1 is a derivative of root 3, and root 2 is a derivative of root 4.

When applying these criteria to the Euglenozoa, the “ventral or posterior flagellum” is indeed F1 and the “dorsal or anterior flagellum” is F2 (Moestrup 2000). However, the “intermediate root” in euglenozoans is root 1, the “ventral root” is root 2, and the single “dorsal root” is root 3. The transformational homology of root 1 and root 3 (see above) is consistent with the model of euglenid cytoskeletal organization described in Yubuki and Leander (2012). This labelling of the roots differs from Moestrup (2000), where the Euglenozoan ventral root is treated as root 1, the intermediate root as root 2, and the dorsal root as root 4.

Our SEM data on dividing *K. bialata* provides the first clear documentation of flagellar transformation in a typical excavate. The posterior flagellum, F1, is older than the anterior flagellum, F2. This is consistent with the developmental pattern reported for the non-typical excavate *Giardia* (Nohýnková et al. 2006). The posterior basal body 1 (B1) has two microtubular roots (and a singlet root) and these can now be identified with confidence: the ‘left root’ which originates from the left side of B1 is root 1 (R1), and the ‘right root’ which originates from the right side of B1 is root 2 (R2). This is the reverse of the identities in Simpson (2003). Similarly, the solitary root associated with the anterior (and younger) flagellum, F2, which originates from the anterior side of basal body 2 (B2), is identified as root 3 (not R4, as in Simpson, 2003). This terminology can be applied to all other excavates and will facilitate more consistent and accurate comparative ultrastructural analyses within the group and with other eukaryotes.

### Comparison of *K. bialata* with Related Taxa

The general ultrastructure of *Kipferlia bialata* was broadly similar to that of other CLOs. It showed the ‘typical excavate’ pattern of flagellar microtubular roots, non-microtubular roots, and a vaned posterior flagellum (Simpson 2003). In particular *K. bialata* possessed an arched B fiber that extended from R1 to R2 against B1, which is a synapomorphy for Fornicata that is shared by all fornicates other than diplomonads (Park et al. 2009, 2010; Simpson 2003; Yubuki et al. 2007). It also possessed rounded MROs without cristae, similar to all other CLOs except *Carpediemonas*, in which the MRO is elongate (Simpson and Patterson 1999).

*Kipferlia bialata* also displayed several distinctive features. The markedly extended ‘hood’ has never been observed in other CLOs, nor any other typical excavate; the B fibres of *Dysnectes* and

*Ergobibamus* are quite broad, but clearly do not support a separate flap along the right side of cell (Park et al. 2010; Yubuki et al. 2007). The hair-like extensions on the ventral flagellar vane in *K. bialata* have never been observed in any other CLO so far, nor in other typical excavates. The absence of a distinguishable dorsal vane is novel amongst the CLOs and retortamonads studied to date. A single ventral vane is present in the aerobic excavate *Malawimonas jakobiformis* (O’Kelly and Nerad 1999), but this almost certainly represents a convergence, since possession of a ventral vane seems to be ancestral for the Fornicata (see below).

Of especial interest are features that *Kipferlia* shares with some, but not all, other CLOs and retortamonads, especially when those features are considered in a phylogenetic context. Molecular phylogenetic analyses using six protein coding genes plus SSU rDNA sequences invariably place *K. bialata* within a robust monophyletic group otherwise consisting of diplomonads, the CLO *Dysnectes*, and two clades currently both identified as retortamonads (Takishita et al. 2012). Retortamonads (*Retortamonas* and *Chilomastix*) are either commensal or parasitic flagellates in animal hosts. The flagellar apparatus of studied retortamonads is similar in the general orientation of basal bodies, associated roots and paracrystalline material (Bernard et al. 1997; Brugerolle 1973, 1977; Simpson and Patterson 1999). However, retortamonads apparently do not form a monophyletic group in multigene phylogenetic analyses, with *Chilomastix* branching among CLOs while an organism currently identified as a *Retortamonas* is sister to diplomonads (Takishita et al. 2012). The free-living *Dysnectes* forms the sister lineage to the diplomonad-*Retortamonas* clade with strong statistical support, but the analyses do not strongly resolve the branching order among *K. bialata*, *Chilomastix*, and the diplomonad/*Retortamonas*/*Dysnectes* clade (Fig. 10).

Takishita et al. (2012) could not nominate morphological traits that would reinforce the molecular phylogenetic relationships among *Dysnectes*, *Retortamonas*, diplomonads, other CLOs, and *Chilomastix*. After examination of the ultrastructural features reported here, it is still difficult to identify traits uniquely shared by *K. bialata*, *Chilomastix*, and the diplomonad/*Retortamonas*/*Dysnectes* clade. Unfortunately, there is currently no overlap in published TEM data and molecular phylogenetic data for nominal species of *Chilomastix* and *Retortamonas*; for instance, *Chilomastix caulleryi* has been studied only within the context of multigene

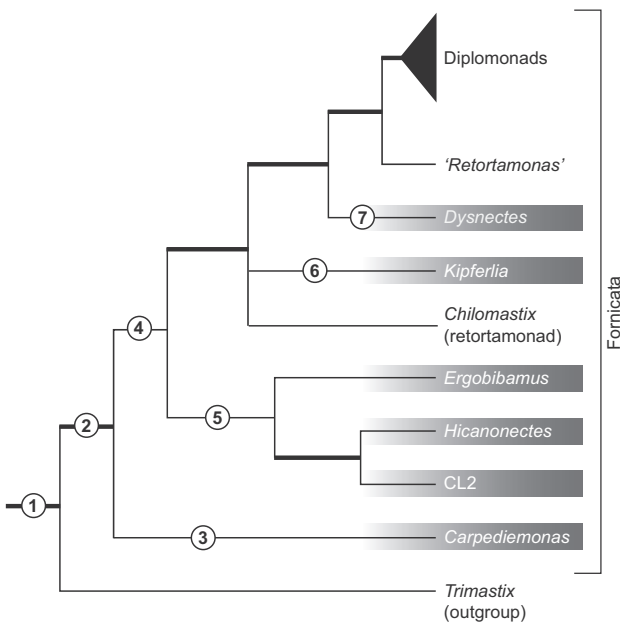


**Figure 10.** A hypothetical phylogenetic framework for understanding the relationships among fornicate lineages as inferred from available molecular and morphological data. The cladogram is modified from Takishita et al. (2012) and the thick branches reflect robust statistical support from their phylogenetic analyses. Shaded lineages are CLOs. *Trimastix* represents the outgroup. See text for discussion.

phylogenetic analyses (Takishita et al. 2012), and *Chilomastix cuspidata*, *Chilomastix aulastomi* and *Retortamonas agilis* have been studied only at the ultrastructural level (Brugerolle 1973, 1977; Bernard et al. 1997). Nonetheless, several of the ultrastructural features reported here in *K. bialata* are reminiscent of those reported in *C. cuspidata* (Bernard et al. 1997). In both species, the deep gutter within the ventral groove separated oR2 and iR2 (syn. “right microtubular band” and “hook-band” in *C. cuspidata*, respectively). The right and left ridges of the gutter were also supported by equivalents of the ODR and an IDR that were closely associated with oR2 and iR2, respectively (Bernard et al. 1997). Deep gutters and structures similar to the ODR and IDR were also imaged in both *C. aulastomi* (where the equivalent of the ODR supported the ‘lateral lamellum’ – see figs 10-12 and 21 in Brugerolle 1973) and in *R. agilis* (figs 8-10 in Brugerolle 1977). Nothing very similar has been seen in other CLOs to date: *Dysnectes* has a very small invagination between at the extreme anterior ends of oR2 and iR2, but neither an ODR nor IDR were observed, and there is no discrete gutter present in the groove proper (Yubuki et al.

2007). A distinct cytopharynx is seen in retortamonads and *Hicanonectes*. In *Chilomastix cuspidata*, an oR2 (right band, RB) and iR2 (hook-band, HB) support the cytopharynx (Bernard et al. 1997) as in *K. bialata*. The presence of four basal bodies has been reported in *Hicanonectes*, *Ergobibamus*, *Chilomastix* spp., and *Retortamonas* (as exemplified by *R. agilis*), while almost all diplomonads have four basal bodies per mastigont (Bernard et al. 1997; Brugerolle 1973, 1977; Brugerolle and Müller 2000; Park et al. 2009, 2010). This contrasts with the presence of three and two basal bodies typically found in *Carpediemonas* and *Dysnectes*, respectively (Simpson and Patterson 1999; Yubuki et al. 2007).

The comb-like structure on the C fiber in *K. bialata* is reminiscent of the C fiber in *Ergobibamus*, although the comb-like projections are less conspicuous in *Ergobibamus* (Park et al. 2010). *K. bialata* and *Dysnectes* are the only CLOs with only one R3 microtubule and without a discrete dorsal fan derived from R3 (Yubuki et al. 2007). *Carpediemonas* has two R3 microtubules and a dorsal fan; *Hicanonectes* and *Ergobibamus* have a dorsal fan and have nine and six R3 microtubules, respectively (Park et al. 2009, 2010; Simpson and Patterson 1999). The A fiber in CLOs consists of short projections associated with dorsal face of oR2. In *Ergobibamus*, the A fiber is a thin element that is also closely associated with iR2, (Park et al. 2010). In *K. bialata*, however, the A fiber is much broader than in any other CLO and consists of a dark round element associated with the iR2.

The typical presence of four basal bodies, a comb-like projection from the C fiber, and a ventral cytopharynx in several CLOs and/or retortamonads is especially noteworthy because these features are also found in the free-living excavate *Trimastix* (Brugerolle and Patterson 1997; O’Kelly et al. 1999; Simpson et al. 2000). *Trimastix* and oxymonads together are the closest relatives of the Fornicata aside from parabasalids (Hampl et al. 2005, 2009) (Fig. 10, position 1); however neither oxymonads nor parabasalids have the excavate feeding groove, and their flagellar apparatuses are relatively derived (although see Simpson et al. 2002). *Trimastix* instead has the ‘typical excavate’ morphology that is more similar to most Fornicata.

### Hypothetical Framework for Fornicate Character Evolution

Detailed ultrastructural data on *Kipferlia*, *Carpediemonas*, *Dysnectes*, *Ergobibamus* and *Hicanonectes* combined with molecular

phylogenetic relationships inferred from multi-gene analyses provide a framework for mapping the evolution of ultrastructural traits within the Fornicata (Takishita et al. 2012) (Fig. 10). The main clades within this framework consist of (1) diplomonads, *Retortamonas*, and *Dysnectes*; (2) the diplomonads/*Retortamonas*/*Dysnectes* clade, *Kipferlia*, and *Chilomastix*; (3) *Hicanonectes* and CL2; and (4) the Fornicata as a whole (Fig. 10).

Using *Trimastix* as an outgroup, we infer that the last common ancestor of Fornicata and *Trimastix* (i.e., of Metamonada) had the following features: a free-living mode of life in low oxygen environments, a ventral feeding groove, two vanes on F1, four basal bodies, reduced and rounded MRO without cristae, a robust R1, a robust oR2, and a dorsal fan that originates in association with R3 (Fig. 10, position 1). R3 was probably relatively small (~4 microtubules or fewer). Based on the likely interrelationships amongst CLOs, diplomonads and retortamonads, parsimony suggests that the most recent common ancestor of the Fornicata was a small biflagellate that lived in marine environments and that possessed an arched B fiber originating from R1 and positioned against the ventral side of B1 (Fig. 10, position 2).

The lineage of *Carpediemonas* saw acquisition of a lateral vane on F1 (independently of *Retortamonas agilis* – see below), loss of one of the interphase basal bodies, a switch from rounded MROs to a more elongate form, and a reduction in the number of microtubules associated with oR2 (Fig. 10, position 3). It is most parsimonious to infer that the dorsal vane on F1 was substantially reduced in the most recent common ancestor of the remaining fornicates (Fig. 10, position 4), though if so, the extended form of the dorsal vane must have evolved again in a common ancestor of true retortamonads, represented by *Chilomastix* (and with the *Retortamonas agilis* lineage also developing a lateral vane, if *R. agilis* proves to be related to *Chilomastix*). The number of microtubules in R3 may have increased in a common ancestor of *Ergobibamus*, *Hicanonectes*, and CL2, if these taxa prove to form a clade (Fig. 10, position 5).

In the absence of sufficient ultrastructural data from *Chilomastix* and from the organisms studied as *Retortamonas*, we are unable to find shared traits for the clade consisting of *Kipferlia*, *Dysnectes*, retortamonads and diplomonads and for the clade consisting of *Dysnectes*, *Retortamonas* and diplomonads (Fig. 10). The hood and a single flagellar vane with terminal hairs on F1 (i.e., complete loss of the dorsal vane) are features that

evolved in *K. bialata* (Fig. 10, position 6). In *Dysnectes*, the number of basal bodies was reduced to two (Fig. 10, position 7). *Kipferlia*, *Dysnectes* and diplomonads lack distinct dorsal fans (Brugerolle 1991; Simpson 2003), whereas the ultrastructure of *Retortamonas*, the sister lineage to diplomonads, is unknown. Therefore, it is possible that the loss of dorsal fans is a synapomorphy for one of the main subclades within the Fornicata. Takishita et al. (2012) inferred that *Hicanonectes* and CL2 share a common ancestor with a similar swimming behavior, an inconspicuous ventral feeding groove, and a curved cytopharynx. Because *K. bialata*, *C. cuspidata*, and *Trimastix* also possess a curved cytopharynx, the origin of this latter feature likely predates the divergence of the *Hicanonectes*-CL2 clade (Fig. 10, position 5). The phylogenetic hypotheses discussed here can be tested and refined as more ultrastructural data from CL2, *Chilomastix*, *Retortamonas*, and more undiscovered isolates from the Fornicata become available.

## Methods

**The culture strain, *Kipferlia bialata* NY0173:** The strain of *Kipferlia bialata* in this study was the same strain reported by Takishita et al. (2007, 2012) and Kolisko et al. (2010) as NY0173. The culture was derived from a sample collected in March 2006 during cruise no. NT06-04 from sea floor sediments at a cold seep site in Sagami bay (1174 m, 35°0'09"N, 139°13'51"E) using the ROV Hyper-Dolphin by JAMSTEC (Japan Agency for Marine-Earth Science and Technology). Cell cultures were maintained at 16°C in seawater with modified TYGM-9 medium (final concentration 5%) under low oxygen conditions. The modified TYGM-9 medium was prepared in accordance with instructions from American Type Culture Collection (ATCC) with two exceptions: the rice starch solution and bovine serum were replaced by rice grains and horse serum, respectively. The culture is deposited in the culture collection at the National Institute for Environmental Studies (NIES, Japan) as strain NIES-1968.

**Light microscopy:** Light microscopy was performed using a Zeiss Axioplan 2 microscope equipped with a Leica DC500 digital camera.

**Scanning electron microscopy:** Cells of *Kipferlia bialata* NY0173 were washed with anoxic seawater several times before being mixed with an equal volume of fixative containing 2.5% (v/v) glutaraldehyde, 0.2 M sucrose or sorbitol and 0.1-1% (w/v) osmium tetroxide in 0.2 M sodium cacodylate buffer (SCB) (pH 7.2). The specimen was centrifuged at 500-650 g for 10 min and mounted on glass plates coated with poly-L-lysine for 1.5 h on ice. The glass plates were rinsed with 0.2 M SCB containing 0.2 M sucrose or sorbitol and fixed in 1% osmium tetroxide for 1 h. The fixed cells were then rinsed with 0.2 M SCB and dehydrated with a graded ethanol series from 30% to absolute ethanol. Samples were critical point dried with CO<sub>2</sub> using a Tousimis critical point dryer. Samples were then coated with gold using a Cressington 208HR high resolution sputter coater, and observed with a Hitachi S-4700 field emission scanning electron microscope.

**Transmission electron microscopy:** For ultra-thin sections, cells were high-pressure frozen using a Leica HPM100. Cells were freeze-substituted in 1% osmium tetroxide and 0.1% uranyl acetate in HPLC grade acetone using a Leica AFS set to -85 °C for three days, warming to -20 °C over 13 h and held at -20 °C for 8 h before warming to 4 °C over 12 h. The cells were washed in acetone, and then increasing concentrations of a 1:1 mixture of JEMBED resin diluted with acetone. The cells were infiltrated with 100% resin at room temperature for 8 hrs. The infiltrated samples were polymerized overnight in resin at 65 °C.

The images shown in Figure 4F and G were derived from a second fixation, in which cells suspended in a mixture of 5% glutaraldehyde and 0.2M sucrose in 0.2M SCB (pH 7.2) at room temperature for one hour. Cells were aggregated into a pellet by centrifugation at 600 g for 10 min, then rinsed with 0.2M SCB (pH 7.2). The suspension was then fixed in 1% osmium tetroxide in 0.2M SCB (pH 7.2) at room temperature for one hour, followed by dehydration through an ethanol series and substitution with acetone. The cells were infiltrated with an acetone-resin (Epon 812) mixture and ultimately embedded in absolute resin. The cells prepared with freeze substitution were generally better fixed than the chemically fixed cells, except for the membranes (e.g., mitochondria).

Serial ultra-thin sections were cut on a Leica EM UC6 ultramicrotome and double stained with 2% (w/v) uranyl acetate and lead citrate (Reynolds 1963). The ultra-thin sections were observed using a Hitachi H7600 electron microscope or Tecnai 12 transmission electron microscope fitted with a goniometer stage.

## Acknowledgements

Dr. Kiyotaka Takishita (JAMSTEC, Japan) provided us with the deep-sea sediment. This research was supported by grants from the Tula Foundation (Centre for Microbial Diversity and Evolution) and the Canadian Institute for Advanced Research, Program in Integrated Microbial Biodiversity.

## References

- Andersen RA** (1991) The cytoskeleton of chromophyte algae. *Protoplasma* **164**:143–159
- Beech PL, Heimann K, Melkonian M** (1991) Development of the flagellar apparatus during the cell cycle in unicellular algae. *Protoplasma* **164**:23–37
- Bernard C, Simpson AGB, Patterson DJ** (1997) An ultrastructural study of a free-living retortamonad, *Chilomastix cuspidata* (Larsen & Patterson, 1990) n. comb. (Retortamonadida, Protista). *Eur J Protistol* **33**:254–265
- Berney C, Fahrni J, Pawlowski J** (2004) How many novel eukaryotic “kingdoms?” Pitfalls and limitations of environmental DNA surveys. *BMC Biol* **2**:13
- Brugerolle G** (1973) Etude ultrastructurale du trophozoïte et du kyste chez le genre *Chilomastix* Alexeieff, 1910 (Zoomastigophorea, Retortamonadida Grassé, 1952). *J Protozool* **20**:574–585
- Brugerolle G** (1977) Ultrastructure du genre *Retortamonas* Grassi 1879 (Zoomastigophorea, Retortamonadida Wenrich 1931). *Protistologica* **13**:233–240
- Brugerolle G** (1991) Flagellar and cytoskeletal systems in amitochondrial flagellates: Archamoeba, Metamonada, and Parabasala. *Protoplasma* **164**:70–90
- Brugerolle G, Müller M** (2000) Amitochondriate Flagellates. In Leadbeater SC, Green JC (eds) *The Flagellates. Unity, Diversity and Evolution*. Taylor & Francis Ltd, London, pp 166–189
- Brugerolle G, Patterson D** (1997) Ultrastructure of *Trimastix convexa* Hollande, an amitochondriate anaerobic flagellate with a previously undescribed organization. *Eur J Protistol* **33**:121–130
- Cavalier-Smith T** (1983) A Six Kingdom Classification and a Unified Phylogeny. In Schwemmler W, Schenk HEA (eds) *Endocytobiology II*. De Gruyter, Berlin, pp 1027–1034
- Edgcomb VP, Kysela DT, Teske A, de Vera Gomez A, Sogin ML** (2002) Benthic eukaryotic diversity in the Guaymas Basin hydrothermal vent environment. *Proc Natl Acad Sci USA* **99**:7658–7662
- Embley TM, Martin W** (2006) Eukaryotic evolution, changes and challenges. *Nature* **440**:623–630
- Hampf V, Simpson AGB** (2008) Possible Mitochondria-related Organelles in Poorly-Studied “Amitochondriate” Eukaryotes. In Tachezy J (ed) *Hydrogenosomes and Mitosomes: Mitochondria of Anaerobic Eukaryotes*. Microbiology Monographs 9. Springer Verlag, Berlin, pp 256–282
- Hampf V, Horner DS, Dyal P, Kulda J, Flegr J, Foster PG, Embley TM** (2005) Inference of the phylogenetic position of oxymonads based on nine genes: support for Metamonada and Excavata. *Mol Biol Evol* **22**:2508–2518
- Hampf V, Hug L, Leigh JW, Dacks JB, Lang BF, Simpson AGB, Roger AJ** (2009) Phylogenomic analyses support the monophyly of Excavata and resolve relationships among eukaryotic “supergroups”. *Proc Natl Acad Sci USA* **106**:3859–3864
- Hjort K, Goldberg AV, Tsaousis AD, Hirt RP, Embley TM** (2010) Diversity and reductive evolution of mitochondria among microbial eukaryotes. *Philos Trans R Soc B* **365**:713–727
- Kolisko M, Silberman JD, Cepicka I, Yubuki N, Takishita K, Yabuki A, Leander BS, Inouye I, Inagaki Y, Roger AJ, Simpson AGB** (2010) A wide diversity of previously undetected free-living relatives of diplomonads isolated from marine/saline habitats. *Environ Microbiol* **12**:2700–2710
- Lee WJ** (2002) Some free-living heterotrophic flagellates from marine sediments of Incheon and Ganghwa Island, Korea. *Korean J Biol Sci* **6**:125–143
- Lee WJ** (2006) Some free-living heterotrophic flagellates from marine sediments of tropical Australia. *Ocean Sci J* **41**:75–95
- Lee WJ, Patterson DJ** (2000) Heterotrophic flagellates (Protista) from marine sediments of Botany Bay, Australia. *J Nat Hist* **34**:483–562
- Moestrup Ø** (1982) Flagellar structure in algae: a review, with new observations particularly on the Chrysophyceae, Phaeophyceae (Fucophyceae), Euglenophyceae and *Reckertia*. *Phycologia* **21**:427–528

- Moestrup Ø** (2000) The Flagellate Cytoskeleton: Introduction of a General Terminology for Microtubular Flagellar Roots in Protists. In Leadbeater SC, Green JC (eds) *The Flagellates. Unity, Diversity and Evolution*. Taylor & Francis Ltd, London, pp 69–94
- Nohýnková E, Tůmová P, Kulda J** (2006) Cell division of *Giardia intestinalis*: Flagellar developmental cycle involves transformation and exchange of flagella between mastigonts of a diplomonad cell. *Eukaryot Cell* **5**:753–761
- O’Kelly CJ** (1993) The jakobid flagellates: structural features of *Jakoba*, *Reclinomonas* and *Histiona* and implications for the early diversification of eukaryotes. *J Eukaryot Microbiol* **40**:627–636
- O’Kelly CJ, Nerad TA** (1999) *Malawimonas jakobiformis* n. gen., n. sp. (Malawimonadidae n. fam.): A *Jakoba*-like heterotrophic nanoflagellate with discoidal mitochondrial cristae. *J Eukaryot Microbiol* **46**:522–531
- O’Kelly CJ, Farmer MA, Nerad TA** (1999) Ultrastructure of *Trimastix pyriformis* (Klebs) Bernard et al.: Similarities of *Trimastix* species with retortamonad and jakobid flagellates. *Protist* **150**:149–162
- Park JS, Kolisko M, Simpson AGB** (2010) Cell morphology and formal description of *Ergobibamus cyprinoides* n. g., n. sp., another *Carpediemonas*-like relative of diplomonads. *J Eukaryot Microbiol* **57**:520–528
- Park JS, Kolisko M, Heiss AA, Simpson AGB** (2009) Light microscopic observations, ultrastructure, and molecular phylogeny of *Hicanonectes teleskopos* n. g., n. sp., a deep-branching relative of diplomonads. *J Eukaryot Microbiol* **56**:373–384
- Philippe H, Germot A** (2000) Phylogeny of eukaryotes based on ribosomal RNA: long-branch attraction and models of sequence evolution. *Mol Biol Evol* **17**:830–834
- Philippe H, Lopez P, Brinkmann H, Budin K, Germot A, Laurent J, Moreira D, Müller M, Guyader HL** (2000) Early-branching or fast-evolving eukaryotes? An answer based on slowly evolving positions. *Proc R Soc B* **267**:1213–1221
- Reynolds ES** (1963) The use of lead citrate at high pH as an electron-opaque stain in electron microscopy. *J Cell Biol* **17**:208–212
- Roger AJ, Sandblom O, Doolittle WF, Philippe H** (1999) An evaluation of elongation factor 1alpha as a phylogenetic marker for eukaryotes. *Mol Biol Evol* **16**:218–233
- Ruinen J** (1938) Notizen über Salzflagellaten. II. Über die Verbreitung der Salzflagellaten. *Arch Protistenkd* **90**:210–258
- Simpson AGB** (2003) Cytoskeletal organization, phylogenetic affinities and systematics in the contentious taxon Excavata (Eukaryota). *Int J Syst Evol Microbiol* **53**:1759–1777
- Simpson AGB, Patterson DJ** (1999) The ultrastructure of *Carpediemonas membranifera* (Eukaryota) with reference to the “Excavate hypothesis”. *Eur J Protistol* **35**:353–370
- Simpson AGB, Bernard C, Patterson DJ** (2000) The ultrastructure of *Trimastix marina* Kent, 1880 (Eukaryota), an excavate flagellate. *Eur J Protistol* **36**:229–251
- Simpson AGB, Radek R, Dacks JB, O’Kelly CJ** (2002) How oxymonads lost their groove: an ultrastructural comparison of *Monocercomonoides* and excavate taxa. *J Eukaryot Microbiol* **49**:239–248
- Sleigh MA** (1988) Flagellar root maps allow speculative comparisons of root patterns and of their ontogeny. *BioSystems* **21**:277–282
- Sogin ML** (1991) Early evolution and the origin of eukaryotes. *Curr Opin Genet Dev* **1**:457–463
- Sogin ML, Gunderson JH, Elwood HJ, Alonso RA, Peattie DA** (1989) Phylogenetic meaning of the kingdom concept: an unusual ribosomal RNA from *Giardia lamblia*. *Science* **243**:75–77
- Takishita K, Yubuki N, Kakizoe N, Inagaki Y, Maruyama T** (2007) Diversity of microbial eukaryotes in sediment at a deep-sea methane cold seep: surveys of ribosomal DNA libraries from raw sediment samples and two enrichment cultures. *Extremophiles* **11**:563–576
- Takishita K, Kolisko M, Komatsuzaki H, Yubuki A, Inagaki Y, Cepicka I, Smejkalová P, Silberman JD, Hashimoto T, Roger AJ, Simpson AGB** (2012) Multigene phylogenies of diverse *Carpediemonas*-like organisms identify the closest relatives of “amitochondriate” diplomonads and retortamonads. *Protist* **163**:344–355
- Tovar J, León-Avila G, Sánchez LB, Sutak R** (2003) Mitochondrial remnant organelles of *Giardia* function in iron-sulphur protein maturation. *Nature* **426**:172–176
- Yubuki N, Leander BS** (2012) Reconciling the bizarre inheritance of microtubules in complex (euglenid) microeukaryotes. *Protoplasts* **249**:859–869
- Yubuki N, Inagaki Y, Nakayama T, Inouye I** (2007) Ultrastructure and ribosomal RNA phylogeny of the free-living heterotrophic flagellate *Dysnectes brevis* n. gen., n. sp., a new member of the Fornicata. *J Eukaryot Microbiol* **54**:191–200

Available online at [www.sciencedirect.com](http://www.sciencedirect.com)

**SciVerse ScienceDirect**